J Nanopart Res (2012) 14:1082
DOI 10.1007/s11051-012-1082-3

RESEARCH PAPER

Investigation on the effect of atomic defects on the breaking behaviors of gold nanowires

Fenying Wang · Wei Sun · Hongbo Wang · Jianwei Zhao · Manabu Kiguchi · Changqing Sun

Received: 5 February 2012 / Accepted: 19 July 2012

Abstract The mechanical properties and breaking behaviors of the [100]-oriented single-crystal gold nanowires containing a set of defect ratios have been studied at different temperatures using molecular dynamics simulations. The size of the nanowire is 10a × 10a × 30a (a stands for lattice constant, 0.408 nm for gold). The mechanical strengths of the nanowires decrease with the increasing temperature. However, the defects that enhance the local thermal energy have improved the nanowire mechanical strength under a wide range of temperature. Comparing to the single-crystal nanowire, the existence of the atomic defects extends the elastic deformation showing a larger yield strain. By summarizing 300 samples at each temperature, the statistical breaking position distribution shows that the nanowire breaking behavior is sensitive to the atomic defects when the defect ratio is 5 % at 100 K, whereas the ratio is 1 % when temperatures are 300 and 500 K.

Keywords Defects · Gold nanowires · The most probable breaking position · Molecular dynamics simulations

Electronic supplementary material The online version of this article (doi:10.1007/s11051-012-1082-3) contains supplementary material, which is available to authorized users.

F. Wang
Education Center for Basic Chemistry Experiments, School of Science, Nanchang University, Nanchang 330031, People's Republic of China

F. Wang
School of Material Science and Engineering, Nanchang University, Nanchang 330031, People's Republic of China

F. Wang · W. Sun · H. Wang · J. Zhao (✉)
State Key Laboratory of Analytical Chemistry for Life Science, School of Chemistry and Chemical Engineering, Nanjing University, Nanjing 210008, People's Republic of China
e-mail: zhaojw@nju.edu.cn

M. Kiguchi
Department of Chemistry, Graduate School of Science, Tokyo Institute of Technology, Tokyo 1528551, Japan

C. Sun
School of Electrical and Electronic Engineering, Nanyang Technological University, Singapore 639798, Singapore

Introduction

In recent years, mechanical properties of the metallic nanowires are of considerable interests due to their potential applications in electronic and electromechanical devices (Wu et al. 2005; Diao et al. 2003; Kruzic 2009; Hemker 2004). The mechanical strength and breaking behavior/failures of nanowires subjected to uniaxial stretching could be affected by many factors, such as stretching rates (Ikeda et al. 1999; Wang et al. 2007), size (Gu et al. 2007; Pastor-Abia et al. 2011), defects (Deng and Sansoz 2009; Gai and

Published online: 11 August 2012

Harmer 2002), crystalline orientation (Wang et al. 2011a), and temperature (Gu et al. 2007; Sankaranarayanan et al. 2007). With experimental methods, mechanical measurements of individual nanowires are challenging, principally owing to some difficulties in performing standard tensile or bending tests on the nanoscale systems (Tsutsui et al. 2010; Yanson et al. 2005). It is also a problem to study the deformation mechanisms, mechanical strength, and breaking behavior of the nanowire containing different defects ratios at different measuring conditions. Theoretical simulations, especially for molecular dynamics (MD) simulations (Allen and Tildesley 1997; Rapaport 2004), have been demonstrated to be powerful to evaluate the properties of nanowires subjected to mechanical stretching. With MD simulations, a profound understanding about mechanical properties of the nanowire will be helpful for designing, manufacturing, and manipulating the metallic nanowire before the nanowire is successfully incorporated into the active component of nanoelectromechanical system (NEMS) devices (Husain et al. 2003; Lieber 2003).

With MD simulations, Lucas et al. (2008) studied the plastic deformation of the silver nanowire and compared with the atomic force microscope (AFM) nanoindentation, indicating that mechanical behaviors of the nanowires corresponded to nucleation and movement of dislocations in the deformation process of the nanowire subjected to tension. Ju et al. (2004) studied the mechanical properties of the ultrathin gold nanowires at different temperatures and gave the influence of temperature on the detected one atom chain. Pastor-Abia et al. (2011) analyzed the abnormal stress drop at the yield point of aluminum nanowires at different sizes and temperatures, and proposed that increasing temperatures could significantly reduce their mechanical strengths. For the properties of metallic nanowires, defects in nanowires were also demonstrated in previous work. Deng and Sansoz (2009) discovered that special defect could be utilized to approach the near-ideal strength in gold nanowires through microstructural design. Moreover, the deformation behavior of the nanowire was found to be sensitive to atomic defects, and it was related with the defect ratio at different strain rates (Wang et al. 2011b) and different temperatures (Wang et al. 2011c). However, less report focused on the defect effect of the whole breaking process together with the mechanical properties of the metallic nanowires (Deng and Sansoz 2009; Lu et al. 2010).

The breaking behavior of metallic nanowires has been found to present a statistic feature (Wang et al. 2007, 2011a, b, c; Liu et al. 2009). After summarizing enormous samples, the breaking positions can be plotted in a histogram, which follows a Gaussian distribution. The peak corresponds to the most probable breaking position (MPBP), which describes the concentration of the stress (Wang et al. 2007, 2011b, c; Liu et al. 2009). These results indicate that analyzing of enormous samples might be the only way to investigate the material failure in the nanoscale devices. Here, different initial equilibrium states were designed to statistically study the breaking behaviors of the [100]-oriented single-crystal gold nanowires subjected to uniaxial stretching at different defect ratios and temperatures.

Methodology

As shown in Fig. 1, the single-crystal gold nanowire was generated as a regular lattice of face-centered cubic (FCC) along the [100] crystallographic orientation. The size of the nanowire was $10a \times 10a \times 30a$ (a stands for lattice constant, 0.408 nm for gold), corresponding to 12,000 atoms. Ten different temperatures were set from 5 to 750 K. At each temperature, 300 initial equilibrium states with different atomic configuration were adopted for the nanowire using different and enough relax time, which were appropriate to ensure the reliability of MD simulations (Wang et al. 2007). In the uniaxial tensile directions (z-direction) of the nanowire, stretching was applied by uniformly moving two fixed layers with a constant strain rate of 1.0 % ps^{-1}. The strain rate is high for any materials and structures from macroscopic viewpoint. However, this region of strain rate could be considered as quasi-static state for the nanoscale materials, and it could avoid the strain rate effects as much as possible (Wang et al. 2007, 2011a, b).

Using statistical analysis, the MPBP is obtained from the fitting peak of breaking position distribution of the perfect single-crystal gold nanowire, and then the position of single-layer defect was constructed in the gold nanowire according to the MPBP of the perfect nanowire (Wang et al. 2011a, b, c). In this work (Fig. 1), the MPBP of the perfect nanowire is around 0.2 or 0.8 in the normalized nanowire at each

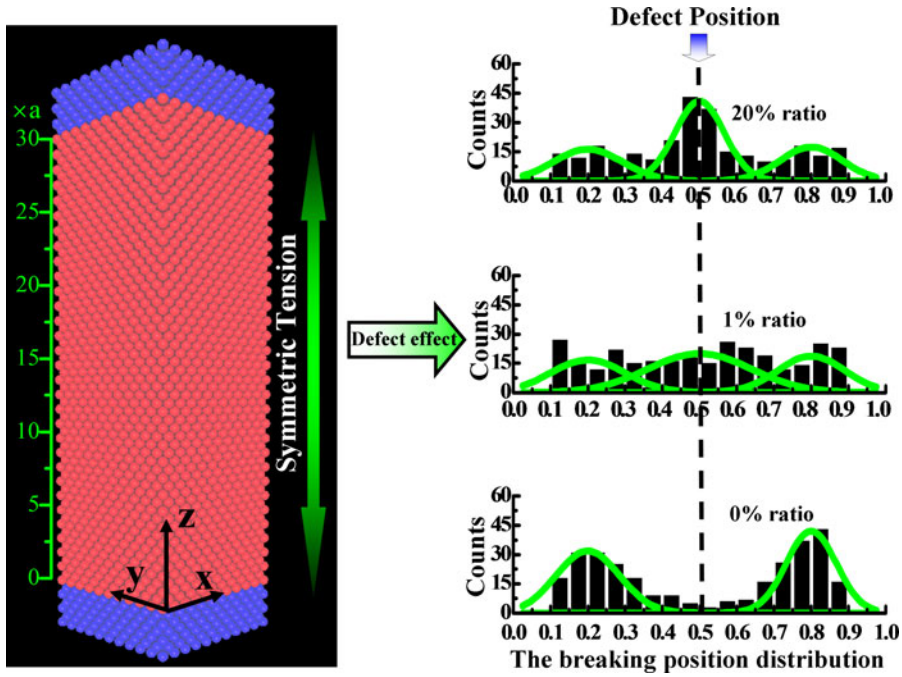

Fig. 1 Schematic illustration of theoretical models. The single-crystal gold nanowire is set as 10a × 10a × 30a (*a* stands for lattice constant, 0.408 nm for gold), corresponding to 12,000 atoms

temperature, and the position of single-layer defect was constructed in the central plane of the nanowire (0.5 in the normalized nanowire). In the single-layer crystalline plane, vacancy defects were constructed to be in a uniform distribution according to vacancy ratio (Wang et al. 2011c). Using this treatment, defect atoms evenly distributed as possible with increasing vacancy ratio. Here, vacancy ratio was defined as the number of vacancies over all atoms in a layer. It varies from 1 to 35 % at 100 K and from 1 to 30 % at 300 and 500 K, respectively. At different temperatures, the last vacancy ratios were set in accord with the influence of defects on the absolute breaking of the nanowires. Table 1 gives the detailed conditions. 8,700 (29 × 300) samples were simulated to give an insight into the defect and the temperature effect on the mechanical properties and breaking behavior of single-crystal gold nanowires.

In MD calculations, the Verlet leapfrog algorithm was applied for the integration of motion equations to obtain velocity and trajectories of atoms with a simulation time step of 1.6 fs (Finbow et al. 1997) Nośe–Hoover thermostat (Nośe 1984a, b; Hoover 1985) used as a rescaling method of velocity. Free boundary condition was adopted. For potential functions, tight-binding molecular dynamics (TB-MD) (Mehl and Papaconstantopoulos 1996; da Silva et al. 2001) or Car-Parrinello molecular dynamics (CP-MD) (Hutter and Curioni 2005) simulations can give accurate results. However, these potential functions have some difficulty in calculating the nanowires with large size or many samples. Therefore, the embedded-atom method (EAM) potential developed by Johnson (Johnson 1989) might be the best choice for this particular purpose. Here, a statistical analysis and a series of comparisons were applied in the present study, which may also reduce the systematic error to ensure the reliability of MD simulations. The EAM potential developed by Johnson followed as:

Table 1 The simulated conditions of the nanowires

Nos.	1	2	3	4	5	6	7	8	9	10
T (K)	5	50	100	150	200	300	500	600	700	750
Ratio (100 K, %)	1	5	10	20	25	30	35			
Ratio (300 K, %)	1	5	10	20	25	30				
Ratio (500 K, %)	1	5	10	20	25	30				

$$E = \frac{1}{2}\sum_{ij} V(r_{ij}) + \sum_{i} F(\rho_i) \quad (1)$$

$$\rho_i = \sum_{i \neq j} \varphi(r_{ij}) \quad (2)$$

where E is the total internal energy of the system, V is the pair potential between atoms i and j, r_{ij} is the distance between them, $F(\rho_i)$ is the energy to embed atom i in an electron density ρ_i, and $\varphi(r_{ij})$ is the electron density at atom i due to atom j as a function of the distance r_{ij}. The stress (σ) in z-direction was calculated by the Virial scheme (Wu 2006) as following:

$$\sigma_i^{zz} = \frac{1}{\Omega_i}\left\{-m_i v_i^z v_i^z + \frac{1}{2}\sum_{j \neq i}\left[\frac{\partial \phi}{\partial r_{ij}} + \left(\frac{\partial F}{\partial \rho_i} + \frac{\partial F}{\partial \rho_j}\right)\frac{\partial f}{\partial r_{ij}}\right]\frac{r_{ij}^z r_{ij}^z}{r_{ij}}\right\} \quad (3)$$

where σ_i^{zz} is the stress tensor of atoms α in the tensile direction (z axis), Ω_i is the volume of i atoms, m is the mass, and v_i^z is the velocity component of atom i in the z direction. In the above scheme, ϕ, F, ρ, and f are from EAM potential (Johnson 1989). They correspond to the pair potential, the embedded energy, the electron density between the atom i or j and all other atoms, and the electron density in r_{ij} between atomic i and j, respectively. The first and the second terms in the right side of the above equation represent the thermal effect and the atomic interactions, respectively. All presented MD simulations and visualization processes were performed with a self-developed software NanoMD (Zhao et al. 2008b), of which reliability has been validated by a large amount of theoretical simulations (Wang et al. 2007, 2010a, b, 2011a, b, c; Zhao et al. 2009) and the experimental measurements (Zhao et al. 2008a; Jiang et al. 2009).

Results and discussion

The mechanical property at different temperatures

With MD simulations, the uniaxial tension of the perfect [100]-oriented single-crystal gold nanowires are studied at ten different temperatures from 5 to 750 K. Figure 2a gives the representative stress–strain relationships of the nanowires subjected to uniaxial tension at temperatures from 5 to 700 K. The strain (ε) was defined as $\varepsilon = (l - l_0)/l_0$, where l was the current stretching length and l_0 was the length just after relaxation. The stress (σ) in the tensile direction was calculated by the Virial scheme (Wu 2006). With the increasing initial strain, stress increases linearly at different temperatures, and the linear increasing trend could be defined as $\sigma = Y \times \varepsilon$, Y is Young's modulus; σ and ε are the yield stress and the yield strain, respectively. This process corresponds to the elastic deformation of the nanowire. With the increasing strain, an abrupt decrease of the stress is shown in the stress–strain response of the nanowire, indicating the beginning of the plastic deformation of the nanowire. Subsequently, with a decreasing trend, the yield cycle repeats continuously and then it is over. During the whole yielding cycle of the nanowire, the stress–strain curves are smooth at low temperatures, whereas, some "minipeaks" or "wavelets" exhibit at high temperatures. It attributes to the influence of temperature on the mechanical properties and deformation processes of the nanowires.

In addition, it is observed that the first yield stress decreases as the temperature increases (Fig. 2a). When the plastic deformation of the nanowire begins, the drop of the first yield stress also decreases. In order to clearly study these characters, in Fig. 2b–d, we show the average statistical results of the first yield strain (ε_1), the first yield stress (σ_1), and Young's modulus (Y) at different temperatures. The average result is from 300 samples at each temperature, and there are ten temperatures from 5 to 750 K. As shown in Fig. 2b, the first yield strain ε_1 decreases when the temperature increases. From 5 to 100 K, an abrupt decrease is identified and the first yield strains are 0.104 (5 K) and 0.086 (100 K). The linear decreasing trend is in accord with a function of $\varepsilon_1 = 0.104 - (2.057 \times 10^{-4}) \times T$. However, the yield strain fluctuates around 0.085 with its exiting statistical errors in the region from 150 to 500 K. It agrees with a function of $\varepsilon_1 = 0.082 + (9.665 \times 10^{-6}) \times T$. After 500 K, with an increase in the temperature, the strain decreases slowly in keeping with a function of $\varepsilon_1 = 0.096 - (1.781 \times 10^{-5}) \times T$. The bigger strain at low temperature indicates that the nanowire maintains its elastic deformation for long time. Whereas, the smaller strain at high temperature illustrates that the plastic deformation begins quickly, which implies that the deformation of the nanowire is in a fast stage of the atomic damage process at high temperature.

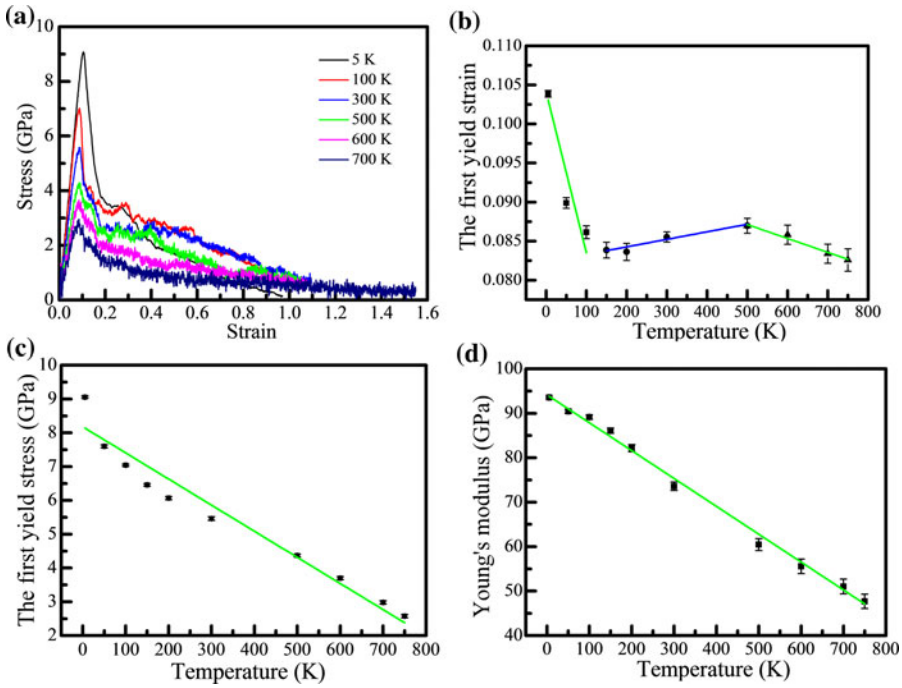

Fig. 2 The mechanical behaviors of the [100]-oriented single-crystal gold nanowires at different temperatures. **a** The representative stress–strain relationship of the nanowire at the temperatures from 5 to 700 K. **b** The first yield strain plotted against temperatures. **c** The first yield stress plotted against temperatures. **d** Young's modulus plotted against temperatures

Such discontinuity in the yield strain also infers the structural change of the nanowire at different temperatures. Here, we named the deformation in the divided range of strain as crystalline, local disorder, and amorphous deformation of the nanowire at three regions of temperatures. In Fig. 2c, d, the first yield stresses and Young's modulus both decrease when the temperature increases. The decreasing behavior of σ_1 accords with a function of σ_1 (GPa) $= 8.179 - 0.008 \times T$, and Young's modulus is Y (GPa) $= 94.14 - 0.063 \times T$. It is observed that the mechanical strength of the metallic material reduces at high temperature and its elastic deformation is prolonged easily at low temperature. Similar temperature dependence of nanowire deformation has also been observed in the self-breaking system. By the self-breaking technique, Tsutsui et al. (2010) have observed that the lifetime of Au atomic contacts is long at relative low temperature. All these temperature-dependent mechanical properties indicate different deformation mechanisms at high and low temperature, which are related with the ways of micro-atomic fluctuation at different temperatures.

Videos S1, S2, and S3 (see Supplementary Videos S1–S3) give the representative deformation behaviors of the nanowires subjected to uniaxial tension at 5, 100, and 500 K, respectively. At 5 K (Video S1), the nanowire has relatively perfect crystalline structures with strain increasing. Some slippage planes appear at the initial plastic deformation with only a slight amorphous, and then two necks exhibit along slippage planes till the overall rupture happens in the gold nanowire. The slippage mechanism is the same as that proposed by Finbow et al. (1997). After a crystalline deformation process of the nanowire at 5 K, the deformation of the nanowire is in a local disordered crystalline process when the temperature is 100 K (Video S2). During the plastic deformation, lots of local disordered structures appear along slippage planes, and the breaking necks are at two ends of the nanowires. Whereas, when the temperature increases to 500 K (Video S3), the amorphization structures exhibit in the whole nanowire, and the nanowire completely undergoes an amorphization deformation. Upon further stretching, it breaks at the end of the nanowire.

In atomic views, the change of crystalline structures is related with atomic thermal movements with a certain potential energy. With thermal movements, metallic atoms overcome atomic cohesive energy, and acute atomic fluctuation brings the breaking of metallic bonds. So it causes the disordered crystalline structures with the increasing potential energies of systems. Figure 3 gives the maximum average

potential energy per atom in the tensile deformation and breaking process of the nanowire at different temperatures. The average potential energy almost increases linearly with the increasing temperature, and the increasing trend is in accord with a function of E (eV) $= -1.906 + (8.290 \times 10^{-5}) \times T$; in which, E is the maximum average potential energy per atom, and T is the temperature. It indicates the increasing of the disorder degree of crystalline structures in the deformation process of the nanowire subjected to uniaxial tension at different temperatures. Under such condition, the system with high energy induces the beginning of the plastic deformation of the nanowire, which also brings the lowering of mechanical strength of the nanowire at high temperatures.

The mechanical property at different defect ratios

The mechanical property of the nanowire reflects the styles of atomic thermal movements at different temperatures, which are also affected by vacancy defects. Here, the single-layer vacancy defects are constructed in the middle of the nanowire at 100, 300, and 500 K, respectively. Vacancy ratios are set from 1 to 35 % at 100 K and both from 1 to 30 % at 300 and 500 K. Under these conditions, the uniaxial tensile behaviors of the [100]-oriented single-crystal gold nanowires containing defects are studied to illustrate the influence of vacancy defects on the mechanical properties of nanowires at different temperatures. Figure 4a gives the representative stress–strain response of the gold nanowire with different vacancy ratios at 100 K. In comparison with Fig. 2a, the smoothness of curves almost does not change under different vacancy ratios. In addition, the main difference between Figs. 4a and 2a is that defects obviously improve the first yield stress of the nanowire. It indicates that the "wavelets" of the stress–strain responses are mainly affected by the temperature, and the constructed vacancy defects have improved the mechanical strengths of the nanowires. However, the influences of atomic defects and temperature are dependent in the uniaxial tensile deformation of the nanowires. That is, the constructed defects hinder the dislocation and bring the improvement of the mechanical strengths. When the temperature increases, it induces the disordered crystalline structures, and local thermal energy induced by defects becomes weak in the system with a constant temperature.

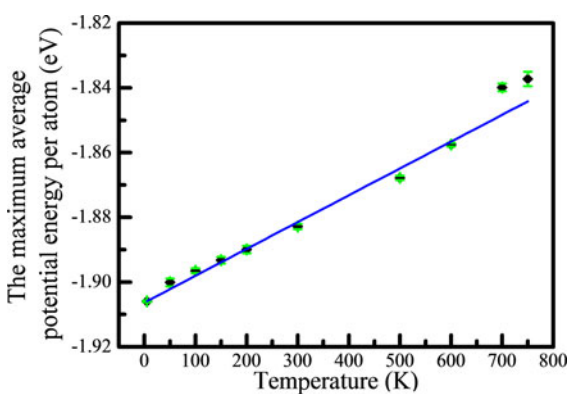

Fig. 3 The maximum average potential energy per atom of the [100]-oriented single-crystal gold nanowire plotted against temperatures

For the influence of vacancy ratios on the first yield properties at the given three temperatures, the relationships between defect ratios and the first yield strain, the first yield stress and Young's modulus, respectively, are shown in Fig. 4b–d. Comparing with the prefect [100]-oriented single-crystal gold nanowire, defects especially for the ratio of 1 % have improved the first yield strains and stresses, and Young's modulus at three temperatures. In detail, when vacancy ratio increases from 0 to 1 % at 100 K, the increasing value of the first yield strain (ΔN1) is 0.013. In contrast, the first yield strain is not sensitive to vacancy defects at 300 and 500 K. It indicates that defects could prolong the elastic deformation of the nanowire at low temperature, which is related with the deformation behaviors at the applied temperature. When defect ratio increases from 0 to 1 % at 100 K, the first yield stress (ΔS1) is 3.67 GPa and Young's modulus (ΔY1) is 24.32 GPa. It illustrates that defects enhance mechanical strengths and bring hardening effects of the nanowires. Comparing with the mechanical strengths at 100 K, the improvements of the first yield stress and Young's modulus at 300 or 500 K not only behave the temperature effects, but also give the influence of defects when vacancy ratio increases from 0 to 1 %. For example, the stress at 300 K (ΔS2) is 2.49 GPa and ΔS3 at 500 K is 2.23 GPa. Young's modulus at 300 K (ΔY2) is 25.07 GPa and ΔY3 at 500 K is 21.98 GPa. It indicates that defects are helpful for improving the mechanical strength within the limitation of defect-induced breaking of the nanowire, which is on the base of the applied temperatures. The improving mechanical strength

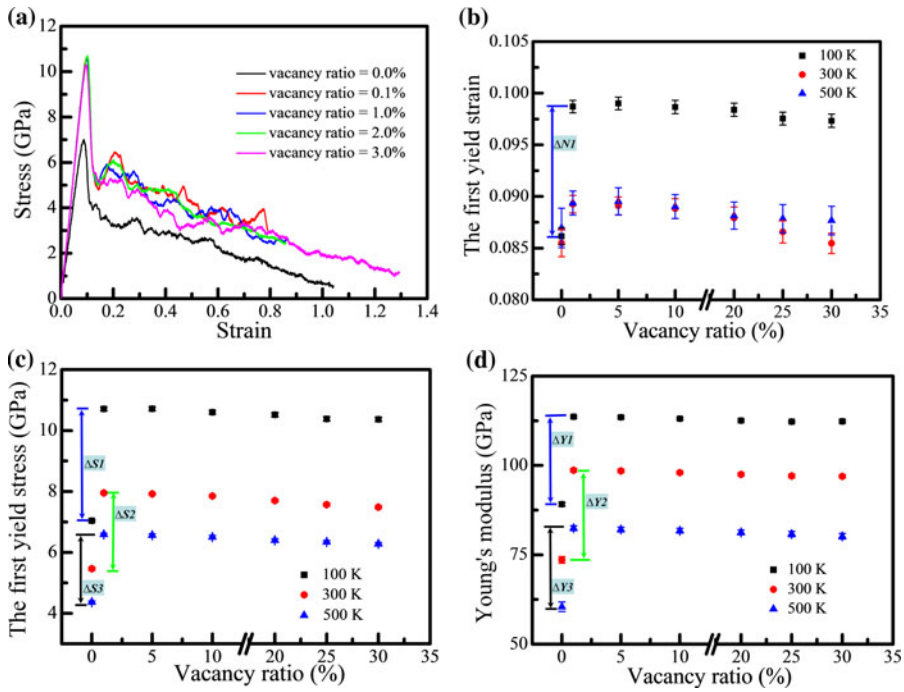

Fig. 4 The mechanical behaviors of the [100]-oriented single-crystal gold nanowires at different vacancy ratios. **a** The representative stress–strain relationship of the nanowire with different vacancy ratios at 100 K. **b** The first yield strain plotted against vacancy ratios. **c** The first yield stress plotted against vacancy ratios. **d** Young's modulus plotted against vacancy ratios. (The defect ratios are from 1 to 30 %.)

attributes to the influence of defects on atomic coordination numbers, which increases the strength of metallic bonds. For such considerations, Pauling (1947) and Goldschmidt (1927) illustrated that the metallic radius of the atom would shrink spontaneously if the coordination number of an atom was reduced. Therefore, coordination number imperfection will shorten the remaining bonds of the under-coordinated atoms and improve the strength of metallic bonds. When the temperature is high, acute microatomic fluctuation induces the amorphization and disordered crystalline structures in the whole nanowire. In contrast, the effect of the constructed atomic vacancies is not obvious for the improvement of the mechanical strength at high temperature. So the sensitivity of the nanowire to vacancies is based on a competition between the vacancies and disordered crystalline structures induced by temperature.

For uniaxial tension-induced deformation of the [100]-oriented single-crystal gold nanowires, the mechanical properties of the nanowire containing defects are related with the deformation behaviors of the nanowires. Defects lower the atomic coordination numbers and induce the breaking of metallic bonds, which increases the strength of metallic bonds. Videos S4 and S5 (see Supplementary Video S4 and S5) give the representative deformation behaviors of the nanowires subjected to uniaxial tension at 100 K with defect ratios of 1 and 30 %, respectively. Comparing with the prefect nanowire in Video S2, S4 shows vacancy defects that delay the appearance of slippage planes when defect ratio is 1 % in the single-layer crystalline plane of the nanowire. The preservation of crystalline structures prolongs the elastic deformation of the nanowire that enhances the mechanical strengths. It corresponds to the improvement of the first yield strain at 100 K. Upon further stretching, the plastic deformation begins and some slippage planes are also observed. With the increasing strain, the necks form along the region of constructed vacancy defects, there is no symmetric distribution at two ends of the nanowire such as Video S2. When vacancy ratio increases to 30 %, Video S5 (see Supplementary Video S5) shows the neck forms in the middle of the nanowire and the nanowire completely breaks around the constructed defect plane. It indicates that defect with a vacancy ratio of 30 % has enough ability to decide the deformation and breaking of the nanowire at 100 K.

It is observed that mechanical properties of the nanowires are different at different temperatures and defect ratios. The defects could prolong the elastic

deformation of the nanowire at low temperature, and mechanical strength of the nanowire can be improved by the constructed defects. That is to say, we can control the temperature and defect ratio to manipulate the deformation characters and mechanical properties of the nanowires in the device designing. Such as the work done by Hu et al. (2012), they designed the super triple junctions in a grain boundary affected zone, and used the finest grains to get the nanocrystalline materials with good strength and good ductility. In addition, Li and Weng (2007) designed a secant-viscosity composite model for the strain-rate sensitivity of nanocrystalline materials. These are undoubtedly helpful for manipulating the material failure in the device designing. For preventing the breaking of the nanowire subjected to uniaxial tension, we could strengthen the nanowire near the breaking regions to avoid its breaking if we have predicted the final breaking positions of the nanowires, which also give insight into mechanical operation of metallic nanowires.

The breaking of the nanowire at different temperatures and defect ratios

Figure 5a shows the breaking position distributions of the [100]-oriented prefect single-crystal gold nanowires at temperatures from 5 to 750 K. The statistical histograms are fitted with Gaussian function, and the fitting peaks replace the most probable breaking position (MPBP) of the nanowires. At each temperature, the most probable breaking positions distribute at two ends of the nanowire. However, the heights of fitting peaks and their widths vary with the applied temperatures, indicating the effect of temperature on the most probable breaking of the nanowires subjected to uniaxial tension. At lower and higher temperatures, the fitting peaks are sharp with higher heights and narrower widths. In contrast, the breaking positions of nanowires behave a dispersed distribution in the middle region of the applied temperatures, and the double fitting peaks have relatively small heights and large widths. Figures S1 and S2 give the widths and heights of peaks against temperatures, respectively. The widths of peaks exhibit an arc-shaped character. Meanwhile, the heights of peaks exhibit an inversed arc-shaped behavior at different temperatures. Macro-breaking position distributions indicate the micro-atomic fluctuations of the nanowires at different temperatures, and the characters of fitting peaks are in consistent with the stretching deformation behaviors of the nanowires at different temperatures. At low temperature of 5 K, micro-atomic fluctuation is in an equilibrium state, and the stretching of the nanowire belongs to crystalline deformation. Upon symmetric stretching, the nanowire breaks easily at two ends and induce macro-breaking position distribution around 0.1 or 0.9 in the normalized nanowire. With the increasing temperature, macro-breaking position distribution becomes wide owing to local disorder crystalline, and the MPBP is at 0.2 or 0.8 in the normalized nanowire. At 700 K, the breaking position distribution transfers again from a dispersed state to a concentrated one in the normalized nanowire. It is because acute micro-atomic fluctuation is in non-equilibrium state at high temperature. The deformation of the nanowire is in an amorphous process, and the damage process of crystalline structures is a fast state. When symmetric tension is applied, a large stress gradient makes the nanowire break at two ends, and then the MPBP distributes at two ends of the nanowire at high temperatures.

In Fig. 5b–d, there are breaking position distributions of the [100]-oriented single-crystal gold nanowires at 100, 300, and 500 K, respectively. The dashed line replaces the position of constructed defects in the single-layer crystalline plane. At 100 K, vacancy ratios are from 1 to 35 %, and at 300 and 500 K, they are from 1 to 30 %, respectively. As shown in Fig. 5b, the breaking position distribution of the perfect nanowire is divided into two parts when vacancy ratio is 0 % at 100 K, which accords with the deformation of the nanowire at the corresponding conditions. The constructed defects in single-layer crystalline plane have affected the breaking position distribution when the ratio is 5 % at 100 K. With the increasing vacancy ratio, the MPBP is gradually moving to the constructed defect position of the nanowire, and the breaking positions completely distribute at the constructed defect position when defect ratio is 35 %. That is, such defect ratio decides the breaking of the nanowire when the temperature is 100 K.

In comparison with the distributions at 100 K, Fig. 5c, d shows that defects with the ratio of 1 % have obviously affected the breaking position distribution of the nanowires when the temperature increases to 300 or 500 K. With the increasing defect ratio, the MPBP moves from two ends (the MPBP of the perfect nanowire at 300 or 500 K) to the middle of the

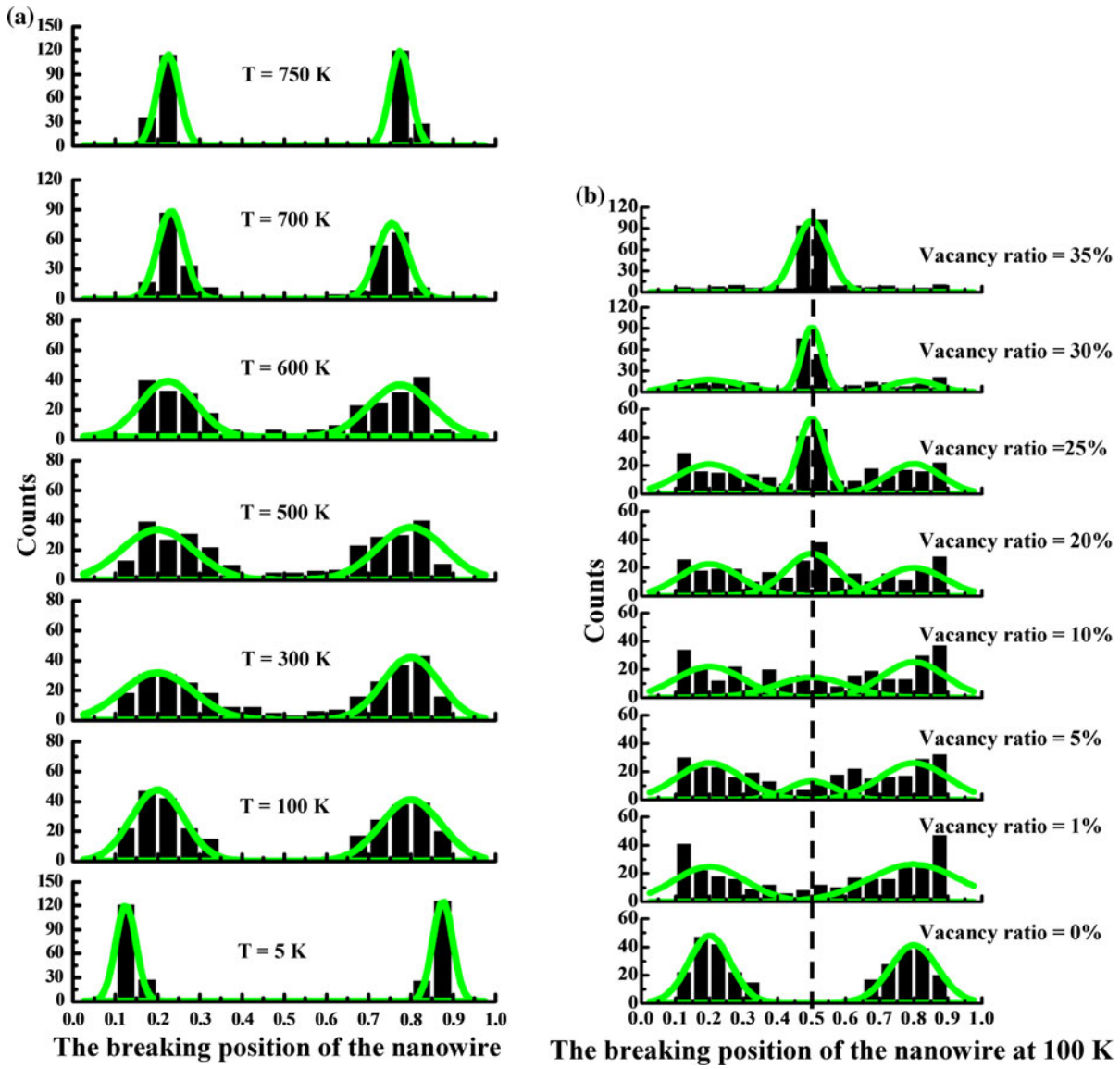

Fig. 5 The breaking position distributions of the [100]-oriented single-crystal gold nanowires. **a** The breaking position distributions of the perfect nanowires at all the simulated temperatures from 5 to 750 K; **b** the breaking position distributions of the nanowires with vacancy ratio from 1 to 35 % at 100 K; **c** the breaking position distributions of the nanowires with vacancy ratio from 1 to 30 % at 300 K; **d** the breaking position distributions of the nanowires with vacancy ratio from 1 to 30 % at 500 K. (The *dash lines* are the constructed defect positions.)

nanowire (the constructed defect position). When defect ratio is 30 %, the MPBP is completely at the constructed defect position, that is 0.5 in the normalized nanowire at 300 and 500 K. From the above comparisons, we could find that the breaking of the nanowire is insensitive to defects at low temperatures. The sensitivity of defects is more obvious with the increasing temperature. It is attributed that the nanowire has longer elastic deformation at low temperature, and the local thermal energy induced by defects becomes weaker in the system with a constant temperature. It results in the insensitivity of defects to the breaking of the nanowire during its plastic deformation at low temperature. Whereas, the plastic deformation begins quickly at high temperature, and local thermal energy induced by defects does

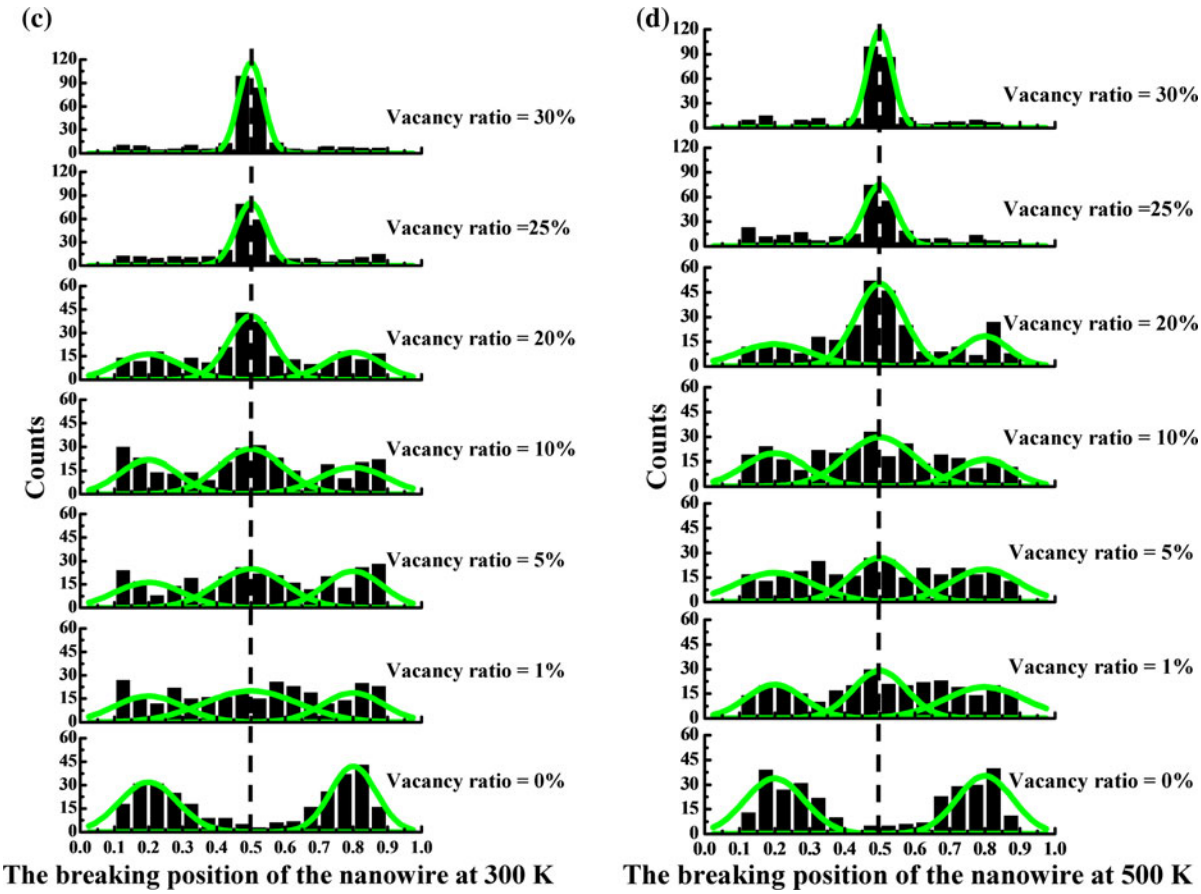

Fig. 5 continued

not have enough time to diffuse in the system. Thus, the defects could affect the deformation of the nanowire, and then the breaking position distribution shows that the breaking of the nanowire is sensitive to defects at high temperature. It is different from previous results that the breaking of the nanowire with small size is sensitive to defects at low temperature (Wang et al. 2011c). It indicates that the nanowire is an unstable high-energy system when the size is small. At low temperature, the crystalline deformation of the nanowire is in a brittle way. Local thermal energy induced by defects is relatively strong in the deformation of the nanowire. Once defects are constructed, crystalline structures will change under uniaxial tension, and then affect the final breaking of the nanowires at low temperature. At high temperature, the system has high potential energy and high kinetic energy under the effects of surface and temperature. Local thermal energy induced by defects plays a less important role in the deformation of the nanowire, which induces the insensitivity of defects to the breaking of the nanowire with small size at high temperature.

Conclusion

The influence of defects and temperature on mechanical properties and the whole breaking process of single-crystal gold nanowire subjected to symmetric stretching were investigated by MD simulations. Several results were obtained as follows: (i) Temperature exhibited a great effect on the mechanical properties of nanowires. The crystalline, local disorder, and amorphous deformations of the nanowires were observed at low, middle, and high temperatures, respectively. (ii) It was observed that defects had improved the mechanical strength of the [100]-

oriented single-crystal gold nanowires. In addition, defects could prolong the elastic deformation of the nanowire at low temperature. (iii) The MPBP distributed at two ends of the nanowire at temperatures from 5 to 750 K. The nanowire breaking was sensitive to the defects, when defects were constructed with the defect ratio 5 % at 100 K. However, the defect ratio was 1 % at 300 and 500 K. It was related with the deformation styles of crystalline structures at different temperatures.

Acknowledgments This project was supported by the National Natural Science Foundation of China (Grant Nos. 20821063, 20873063 and 51071084), National Basic Research Program of China (973 Program, Grant Nos. 2007CB936302 and 2010CB732400), Natural Science Foundation of Jiangsu Province (BK2010389), Fundamental Research Funds for the Central Universities, and Special Postdoctoral Science Foundation funded project of Jiangxi Province.

References

Allen MP, Tildesley DJ (1997) Computer simulation of liquids. Clarendon, New York

da Silva EZ, da Silva AJR, Fazzio A (2001) How do gold nanowires break? Phys Rev Lett 87:256102

Deng C, Sansoz F (2009) Near-ideal strength in gold nanowires achieved through microstructural design. ACS Nano 3:3001–3008

Diao JK, Gall K, Dunn ML (2003) Surface-stress-induced phase transformation in metal nanowires. Nature Mater 2: 656–660

Finbow GM, LyndenBell RM, McDonald IR (1997) Atomistic simulation of the stretching of nanoscale metal wires. Mol Phys 92:705–714

Gai PL, Harmer MA (2002) Surface atomic defect structures and growth of gold nanorods. Nano Lett 2:771–774

Goldschmidt VM (1927) Crystal structure and chemical correlation. Ber Deut Chem Ges 60:1263–1296

Gu MX, Sun CQ, Chen Z, Yeung TCA, Li S, Tan CM, Nosik V (2007) Size, temperature, and bond nature dependence of elasticity and its derivatives on extensibility, Debye temperature, and heat capacity of nanostructures. Phys Rev B 75:125403

Hemker KJ (2004) Understanding how nanocrystalline metals deform. Science 304:221–223

Hoover WG (1985) Canonical dynamics-equilibrium phase-space distributions. Phys Rev A 31:1695–1697

Hu LL, Huo LX, Zhou JQ, Wang Y, Zhang S (2012) The effects of the finest grains on the mechanical behaviours of nanocrystalline materials. J Nanopart Res 14:677–694

Husain A, Hone J, Postma HWC, Huang XMH, Drake T, Barbic M, Scherer A, Roukes ML (2003) Nanowire-based very-high-frequency electromechanical resonator. Appl Phys Lett 83:1240–1242

Hutter J, Curioni A (2005) Car-Parrinello molecular dynamics on massively parallel computers. Chem Phys Chem 6: 1788–1793

Ikeda H, Qi Y, Cagin T, Samwer K, Johnson WL, Goddard WA (1999) Strain rate induced amorphization in metallic nanowires. Phys Rev Lett 82:2900–2903

Jiang LY, Yin X, Zhao JW, Liu HM, Liu YH, Wang FY, Zhu JJ, Boey F, Zhang H (2009) Theoretical investigation on the thermal stability of hollow gold nanoparticles. J Phys Chem C 113:20193–20197

Johnson RA (1989) Alloy models with the embedded-atom method. Phys Rev B 39:12554–12559

Ju SP, Lin JS, Lee WJ (2004) A molecular dynamics study of the tensile behaviour of ultrathin gold nanowires. Nanotechnology 15:1221–1225

Kruzic JJ (2009) Predicting fatigue failures. Science 325: 156–158

Li J, Weng GJ (2007) A secant-viscosity composite model for the strain-rate sensitivity of nanocrystalline materials. Int J Plast 23:2115–2133

Lieber CM (2003) Nanoscale science and technology: building a big future from small things. MRS Bull 28:486–491

Liu YH, Zhao JW, WF Y (2009) The influence of length on shock-induced breaking behavior of copper nanowires. Phys Rev B 80:115417

Lu Y, Huang JY, Wang C, Sun S, Lou Jun (2010) Cold welding of ultrathin gold nanowires. Nature Nanotech 5:218–224

Lucas M, Leach AM, McDowell MT, Hunyadi SE, Gall K, Murphy CJ, Riedo E (2008) Plastic deformation of pentagonal silver nanowires: comparison between AFM nanoindentation and atomistic simulations. Phys Rev B 77: 245420

Mehl MJ, Papaconstantopoulos DA (1996) Applications of a tight-binding total-energy method for transition and noble metals: elastic constants, vacancies, and surfaces of monatomic metals. Phys Rev B 54:4519–4530

Nośe S (1984a) A molecular-dynamics method for simulations in the canonical ensemble. Mol Phys 52:255–268

Nośe S (1984b) A unified formulation of the constant temperature molecular-dynamics methods. J Chem Phys 81: 511–519

Pastor-Abia L, Caturla MJ, SanFabian E, Chiappe G, Louis E (2011) Abnormal stress drop at the yield point of aluminum nanowires: a molecular dynamics study. Phys Rev B 83: 165441

Pauling L (1947) Atomic radii and interatomic distances in metals. J Am Chem Soc 69:542–553

Rapaport DC (2004) The art of molecular dynamics simulation, 2nd edn. Cambridge University Press, Cambridge

Sankaranarayanan SKRS, Bhethanabotla VR, Joseph B (2007) Molecular dynamics simulation of temperature and strain rate effects on the elastic properties of bimetallic Pd-Pt nanowires. Phys Rev B 76:134117

Tsutsui M, Ohshiro T, Matsubara K, Furuhashi M, Taniguchi M, Kawai T (2010) Atomically controlled fabrications of subnanometer scale electrode gaps. J Appl Phys 108: 064312

Wang DX, Zhao JW, Hu S, Yin X, Liang S, Liu YH, Deng SY (2007) Where, and how, does a nanowire break? Nano Lett 7:1208–1212

Wang FY, Liu YH, Yin X, Wang N, Wang DX, Gao YJ, Zhao JW (2010a) The interface and surface effects of the bi-crystal nanowires on their mechanical behaviors under uniaxial stretching. J Appl Phys 108:074311

Wang FY, Liu YH, Zhu TM, Gao YJ, Zhao JW (2010b) Nanoscale interface of metals for withstanding momentary shocks of compression. Nanoscale 2:2818–2825

Wang FY, Gao YJ, Zhu TM, Zhao JW (2011a) Shock-induced breaking of the nanowire with the dependence of crystallographic orientation and strain rate. Nanoscale Res Lett 6:291

Wang FY, Gao YJ, Zhu TM, Zhao JW (2011b) Shock-induced breaking in the gold nanowire with the influence of defects and strain rates. Nanoscale 3:1624–1631

Wang FY, Chen TN, Zhu TM, Gao YJ, Zhao JW (2011c) Uniaxial tension-induced breaking in the gold nanowire with the influence of defects and temperatures. J Appl Phys 110:084307

Wu HA (2006) Molecular dynamics study of the mechanics of metal nanowires at finite temperature. Eur J Mech A-Solids 25:370–377

Wu B, Heidelberg A, Boland JJ (2005) Mechanical properties of ultrahigh-strength gold nanowires. Nature Mater 4: 525–529

Yanson IK, Shklyarevskii OI, Csonka S, van Kempen H, Speller S, Yanson AI, van Ruitenbeek JM (2005) Atomic-size oscillations in conductance histograms for gold nanowires and the influence of work hardening. Phys Rev Lett 95: 256806

Zhao JW, Murakoshi K, Yin X, Kiguchi M, Guo Y, Wang N, Liang S, Liu H (2008a) Dynamic characterization of the postbreaking behavior of a nanowire. J Phys Chem C 112:20088–20094

Zhao JW, Yin X, Liang S, Liu YH, Wang DX, Deng SY, Hou J (2008b) Ultra-large scale molecular dynamics simulation for nano-engineering. Chem Res Chin Univ 24:367–370

Zhao J, Wang F, Jiang L, Yin X, Liu Y (2009) Breaking behavior of a bicrystal copper nanowire studied using a fourier transformation method. Acta Phys Chim Sin 25: 1835–1840